NJC

PAPER

View Article Online
View Journal | View Issue

Check for updates

Cite this: *New J. Chem.*, 2019, **43**, 17211

High conversion of CO_2 into cyclic carbonates under solvent free and ambient pressure conditions by a Fe-cyanide complex†

Pengbo Jiang,‡ Lei Ma,‡ Kaizhi Wang, Kai Lan, Zhenzhen Zhan, Anam Iqbal, Fang Niu and Rong Li *

Received 5th August 2019,
Accepted 15th September 2019

DOI: 10.1039/c9nj04058g

rsc.li/njc

Methods of converting carbon dioxide into valuable chemicals are of great demand but their development is still challenging. Herein, we developed an efficient, green and facile synthetic method for the preparation of a Fe-cyanide complex. The target catalyst showed high catalytic activity for the cyclic reaction of carbon dioxide and epoxide under solvent free conditions and ambient pressure. Meanwhile, the effects of morphology of different catalysts on their catalytic activities were also investigated by the kinetic and thermodynamic studies. In addition, the catalyst could be recycled and reused for at least five successive cycles without significant decrease in the catalytic activity. This target catalyst thus represents one of the efficient and recyclable systems reported for the cyclic reaction in industry.

1. Introduction

Carbon dioxide (CO_2) is regarded as a greenhouse gas and is mainly produced by the combustion of fossil fuels. In recent years, the increasing content of CO_2 in the atmosphere is causing global warming. In response, the utilization of carbon dioxide has attracted considerable research interest in different areas.[1–9] However, in addition to its greenhouse effect, CO_2 also offers a number of advantages: (1) it is inexpensive, (2) easily available and (3) from the carbon-chemical point of view, the carbon in carbon dioxide is renewable.[10,11] Hereby, CO_2 can be used as a raw material to synthesize a variety of highly valuable products such as formamides,[12] methanol,[13] formic acid[14] and cyclic carbonates.[15,16] Cyclic carbonates have been widely applied in the fields of aprotic polar solvents, synthesis of plastics, medicines *etc.*[17–19] The synthesis of cyclic carbonates from CO_2 and epoxides has been widely popular among researchers because of the high atom efficiency (100%) of the cyclic reaction.[20] As a consequence, a number of catalysts including ionic liquids, onium salts and phosphines have been reported.[10,21–24] Furthermore, a variety of heterogeneous catalysts have been investigated for the reaction of CO_2 and epoxides, such as metal salts, metallic oxides and metal–organic frameworks.[25–29] Homogeneous catalysts suffer from high operating costs and cannot be separated easily from the reaction media. However, heterogeneous catalysts could overcome these shortcomings well.

Double metal cyanide (DMC) was first discovered for synthesizing cyclic carbonates from CO_2 and epoxides in 1966.[30] DMC comprises a metal ion (M^1 being an oxophilic metal), which forms a strong bond with oxygen and another metal (M^2 is a transition metal) cyanide salt, *e.g.*,$[M^1]_n[M^2(CN)_6]_m$. Later on, various DMC polytypes were developed as the catalyst for synthesizing cyclic carbonates.[31–36] However, for most DMC, the M^2 is Co and such types of DMC as the catalyst for the synthesis of cyclic carbonates require a higher CO_2 pressure, longer reaction times or higher reaction temperatures.[36]

Herein, we report the synthesis of a Fe-cyanide complex from inexpensive potassium ferricyanide and other metal ions (Fe^{2+}, Zn^{2+}, Ni^{2+}, and Co^{2+}) by a simple and green method. The catalyst shows a high catalytic activity and selectivity (99%) under mild conditions (solvent free, at 100 °C). Moreover, the effect of the morphology of the catalyst on its catalytic activity and the effect of the co-catalyst on the cyclic reaction were investigated by kinetic and thermodynamic studies. Finally, it was found that the catalyst can be recycled for at least five times without significant decrease in activity.

2. Experiment

2.1 Reagents and chemicals

All the reagents and solvents used in the synthesis of the catalyst were purchased from commercial sources and used

---

State Key Laboratory of Applied Organic Chemistry (SKLAOC), the Key Laboratory of Catalytic Engineering of Gansu Province, College of Chemistry and Chemical Engineering, Lanzhou University, Lanzhou, Gansu, 730000, P. R. China. E-mail: liyirong@lzu.edu.cn; Fax: +86-931-8912582; Tel: +86-18919803060

† Electronic supplementary information (ESI) available. See DOI: 10.1039/c9nj04058g

‡ These authors contributed equally to this work and should be considered co-first authors.

without further purification. Ferric(III) nitrate nonahydrate ($Fe(NO_3)_3·9H_2O$, 98.5%), nickel(II) nitrate hexahydrate ($Ni(NO_3)_2·6H_2O$, 98.0%), zinc(II) chloride ($ZnCl_2$, 99.0%) and potassium hexacyanoferrate(II) trihydrate ($K_4[Fe(CN)_6]·3H_2O$) were purchased from Chengdu Kelong Chemical Reagents Co., Ltd. Cobalt(II) nitrate hexahydrate ($Co(NO_3)_2·6H_2O$, 98.5%) was purchased from Shanghai Zhongqin Chemical Reagents Co., Ltd. Ferrous chloride tetrahydrate ($FeCl_2·4H_2O$, 98.5%) was purchased from Xilong Science Chemical Reagents Co., Ltd. Potassium hexacyanoferrate(III) hexahydrate ($K_3[Fe(CN)_6]·6H_2O$) was purchased from Tianjin Guangfu Chemical Reagents Co., Ltd.

2.2 Preparation of the catalyst

For the synthesis of the $Fe_4^{III}(Fe(CN)_6)_3$, $FeCl_2·4H_2O$ (1 mmol) and $K_3[Fe(CN)_6]·6H_2O$ (0.5 mmol) were dissolved in 20 mL of distilled water, separately. The two solutions were mixed with magnetic stirring and the mixture was transferred to a Teflon-lined stainless steel autoclave and heated at 80 °C for 12 h. The resultant solid was collected by centrifugation and washed 3 times with water and dried at 80 °C overnight.

The detailed preparation process of other catalysts (except the Prussian blue micro-cubes) is similar to the above process.

Prussian blue micro-cube, $Fe_4^{III}(Fe(CN)_6)_3$, was prepared by a reported method.[37] Briefly, 0.5 mmol of $K_4Fe(CN)_6·3H_2O$ was added to a HCl solution (0.1 M, 50 mL) under constant magnetic stirring. After stirring for 10 min, a clear solution was obtained. Then, the mixture was transferred to a Teflon-lined stainless steel autoclave and heated at 80 °C for 12 h. The resultant solid was collected by centrifugation and washed 3 times with ultra-pure water and then dried at 80 °C overnight.

2.3 Characterization of the catalysts

The XRD patterns of the catalysts were recorded by an X-ray diffractometer (XRD) Rigaku D/max-2400. The metal content was measured by inductively coupled plasma optical emission spectrometry (ICP-OES), which is carried out on a PerkinElmer (Optima-4300DV) instrument. Scanning electron microscopy (SEM) was performed on a MIRA3 TESCAN instrument. The transmission electron microscopy (TEM), high-resolution transmission electron microscopy (HR-TEM), and high angle annular dark field-scanning transmission electron microscopy (HAADF-STEM) were carried out to investigate the morphology. Nitrogen physisorption isotherms were carried out on a TriStar II 3020 V1.04 instrument. The specific surface area was calculated by the Brunauer–Emmett–Teller method. X-ray photoelectron spectroscopy (XPS) was performed on PHI-5702 instruments.

2.4 Catalytic conversion of CO_2 to cyclic carbonates

The conversion of CO_2 to a cyclic carbonate was carried out in a 25 mL three-necked round bottom flask under reflux and CO_2 bubbling. Epoxide (5 mmol), catalyst (10 mg) and co-catalyst (Bu_4NBr or others) 2.5 mol% were mixed in a three-necked round bottom flask and the reaction mixture was kept in a n oil bath and stirred (600 rpm) for 0.25–5 h. Samples were collected and filtered after the completion of the reaction and the conversion, selectivity and product yield were detected by gas chromatography-mass spectrometry (GC-MS, Agilent 6890N/5937N) and ^1H NMR spectroscopy (Varian Inova 400, 400 MHz using $CDCl_3$ as a solvent).

The activities of the catalysts were calculated as follows: conversion % = $100 \times ([C_0 - C_1]/[C_0])$, selectivity % = $100 \times [C']/[C_0 - C_1]$ and yield % = $100 \times [C']/[C_0]$, where, $[C_0]$ is the initial concentration of the substrate, $[C_1]$ is the concentration of the substrate at the end of the reaction, and $[C']$ is the concentration of the target product at the end of the reaction.

3. Results and discussion

3.1 Characterization of the catalyst

The XRD pattern is shown in Fig. 1a, which shows the crystallinity of catalysts. The XRD curves of catalysts show eight observable peaks at 17.3°, 24.6°, 35.2°, 39.4°, 43.4°, 50.5°, 53.9° and 57.0° corresponding to the lattice planes of (200), (220), (400), (420), (422), (440), (600) and (620) (JCPDS no. 73-0687), respectively.[38] The Raman spectrum is shown in Fig. 1b with two strong peaks at 2091 and 2130 cm^{-1}, indicating the stretching vibration of the carbon nitrogen triple bond.[39] Furthermore, the bands at 264 and 534 cm^{-1} could be assigned to the stretching and bending modes of $Fe–C{\equiv}N–Fe$.[40]

The morphologies and microstructures of the prepared samples were characterized by TEM. TEM images of $Fe_4^{III}(Fe(CN)_6)_3$ (Fig. 2a) show that the synthesized $Fe_4^{III}(Fe(CN)_6)_3$ does not have

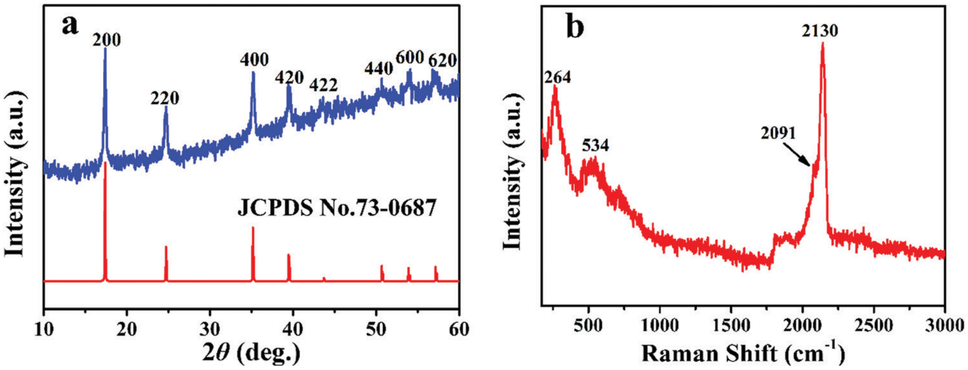

Fig. 1 (a) XRD pattern and (b) Raman spectra of $Fe_4^{III}(Fe(CN)_6)_3$.

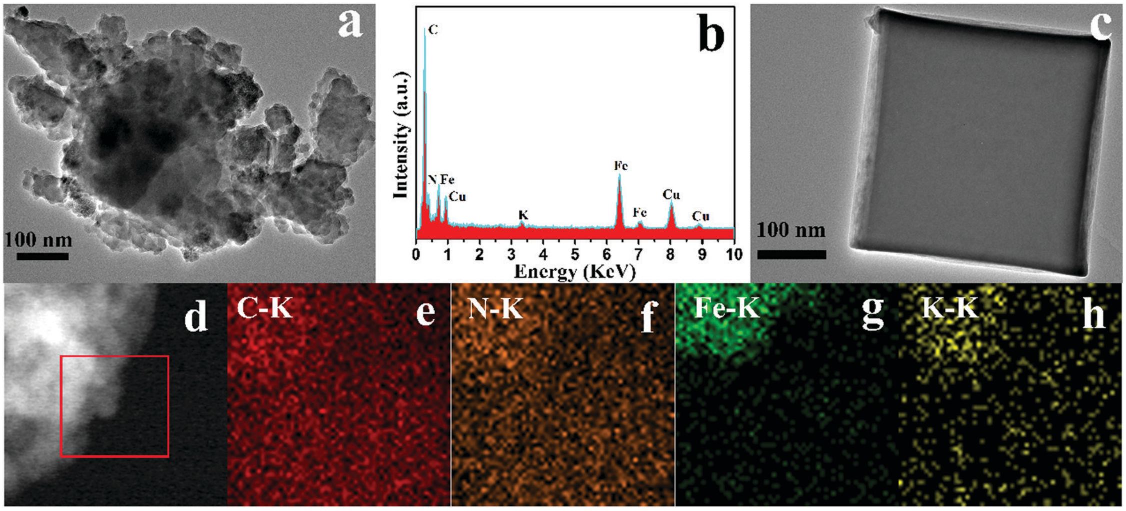

Fig. 2 (a) The TEM image of $Fe_4^{III}(Fe(CN)_6)_3$, (b) the EDX spectrum of $Fe_4^{III}(Fe(CN)_6)_3$, (c) the TEM image of $Fe_4^{III}(Fe(CN)_6)_3$-cube, (d) HAADF-STEM image of $Fe_4^{III}(Fe(CN)_6)_3$, (e–h) elemental mapping of $Fe_4^{III}(Fe(CN)_6)_3$.

a regular structure. To study the elemental distribution of $Fe_4^{III}(Fe(CN)_6)_3$, high angle annular dark field scanning transmission electron microscopy (HAADF-STEM) was performed (Fig. 2d). The energy dispersive X-ray (EDX) elemental mapping (Fig. 2b) analysis indicates a uniform distribution of C, N, K and Fe throughout the entire region. In addition, the data of EDX also provides the molar fraction of elements (C 83.55%, N 10.50%, K 0.33% and Fe 3.39%) in the catalyst. Fig. 2c shows the cubic structure of $Fe_4^{III}(Fe(CN)_6)_3$-cube. Furthermore, the SEM images of the catalyst are shown in Fig. S1 (ESI†) and we found that most of the catalysts have massive structures except the $Fe_4^{III}(Fe(CN)_6)_3$-cube.

Nitrogen adsorption–desorption isotherms of the prepared catalysts were also measured. The isotherms reveal a type-IV adsorption isotherm with the H1 and H3 type hysteresis loop at a high relative pressure (Fig. 3a), indicating a uniform filling of the pores.[41] Furthermore, the surface area and pore volume of $Fe_4^{III}(Fe(CN)_6)_3$ was found to be 296.3 $m^2\ g^{-1}$ and 0.23 $cm^3\ g^{-1}$, respectively. Large surface area and pore volume are responsible for the high catalytic activity of the catalyst.[42,43] The hysteresis loops in the high-pressure region of $Fe_4^{III}(Fe(CN)_6)_3$-cube exhibits that the catalyst does not have a mesoporous structure. The surface area and pore volume of the $Fe_4^{III}(Fe(CN)_6)_3$-cube was 10.0 $m^2\ g^{-1}$ and 0.018 $cm^3\ g^{-1}$, respectively. The $Fe_4^{III}(Fe(CN)_6)_3$-cube catalyst has a solid core cube and this structure is not conducive for active sites contacting with the substrate.

XPS measurements were carried out to further investigate the surface composition and chemical state of the as-prepared catalyst. All the binding energies obtained in the XPS analysis were calibrated using the C1s peak at 284.6 eV. The wide-range XPS spectrum (Fig. 4a) clearly shows that the C1s (284.6 eV), N1s (397.9 eV) and Fe2p (708.5 and 721.8 eV) elements are present on the surface of the catalyst.[44] The high-resolution spectrum of Fe2p (Fig. 4b) shows four main peaks with the binding energy of 708.5, 711.5, 721.4 and 724.3 eV. The peaks located at 708.5 and 724.3 eV correspond to $Fe2p_{3/2}$ and $Fe2p_{1/2}$ of $[Fe^{II}(CN)_6]$,[4–45] while the binding energy of 711.5 and 721.4 eV can be assigned to $Fe^{III}2p_{3/2}$ and $Fe^{III}2p_{1/2}$ in the $Fe_4^{III}(Fe(CN)_6)_3$ catalyst, respectively.[38,44]

3.2 Evaluation of catalysts

Initially, the cycloaddition of styrene oxide with CO_2 (1 atm) to produce styrene carbonate was carried out as the model reaction to test the activity of various catalysts in the presence of TBAB

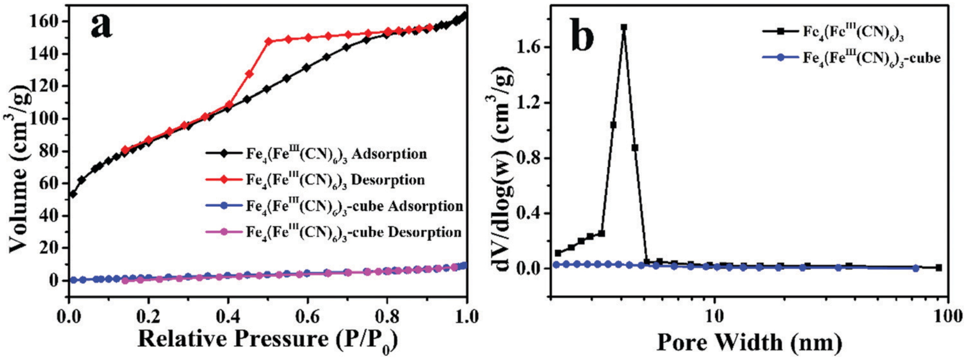

Fig. 3 (a) N_2 adsorption–desorption isotherm of $Fe_4^{III}(Fe(CN)_6)_3$ and $Fe_4^{III}(Fe(CN)_6)_3$-cube, (b) pore volume of $Fe_4^{III}(Fe(CN)_6)_3$ and $Fe_4^{III}(Fe(CN)_6)_3$-cube.

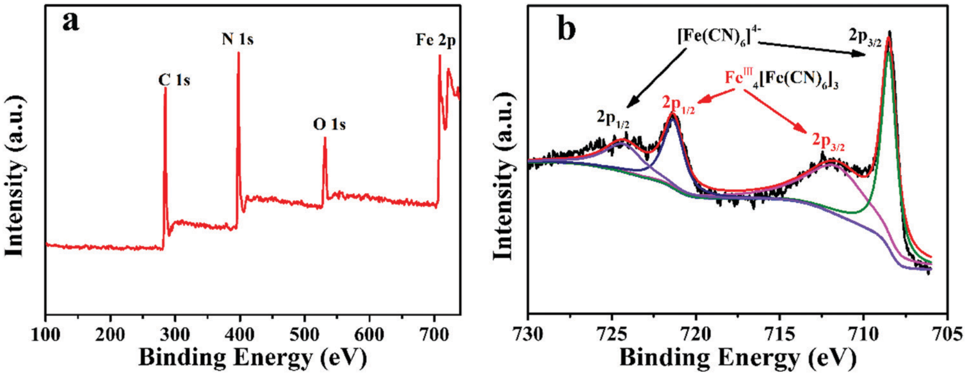

Fig. 4 (a) XPS survey spectrum of all elements present in $Fe_4^{III}(Fe(CN)_6)_3$, (b) the corresponding high-resolution XPS spectra of Fe.

Table 1 The consequence of the reaction of styrene oxide and CO_2 with different catalysts[a]

Entry	Catalysts	Co-catalyst	Temperature (°C)	Conversion (%)	Selectivity (%)	Yield[b] (%)
1	$Fe_4^{III}(Fe(CN)_6)_3$	—	100	0	0	0
2	—	TBAB	100	10	95	9.5
3	$Fe_4^{III}(Fe(CN)_6)_3$	TBAB	100	99	99	99
4	$Fe_4^{III}(Fe(CN)_6)_3$-cube	TBAB	100	85	93	79
5	$KNi_4(Fe^{III}(CN)_6)_3$	TBAB	100	90	96	86
6	$KZn_4(Fe^{III}(CN)_6)_3$	TBAB	100	80	96	76
7	$KCo_4(Fe^{III}(CN)_6)_3$	TBAB	100	65	51	33
8	$Fe_4^{III}(Fe(CN)_6)_3$	TBAC	100	97	95	92
9	$Fe_4^{III}(Fe(CN)_6)_3$	TBAI	100	98	96	94
10	$Fe_4^{III}(Fe(CN)_6)_3$	TBAB	90	90	92	83
11	$Fe_4^{III}(Fe(CN)_6)_3$	TBAB	80	76	89	67
12	$Fe_4^{III}(Fe(CN)_6)_3$	TBAB	70	71	70	49
13	$Fe_4^{III}(Fe(CN)_6)_3$	TBAB	60	60	52	31

[a] Reaction conditions: styrene oxide (5 mmol), 2.5 mol% co-catalyst, catalyst (10 mg), CO_2 pressure (1 atm), reaction time (3 h), conversion and selectivity were determined by GC-MS. [b] The product of styrene carbonate.

(TBAC or TBAI) as co-catalyst, and the results are listed in Table 1. Negligible amounts of the products were detected when the reaction was performed without a co-catalyst (Table 1, entry 1) or when only TBAB (Table 1, entry 2) was used at 100 °C and 1 atm CO_2 pressure. This process indicates that the catalyst and co-catalyst both are essential for the cycloaddition reaction. Entries 3–9 show that different types of catalysts have different catalytic activities. The $Fe_4^{III}(Fe(CN)_6)_3$ catalyst (entry 3) can catalyze the reaction of styrene oxide and CO_2 in the presence of the co-catalyst (TBAB) to attain 99% conversion and 99% selectivity for styrene carbonate. With the TBAC (entry 8) or TBAI (entry 9) as

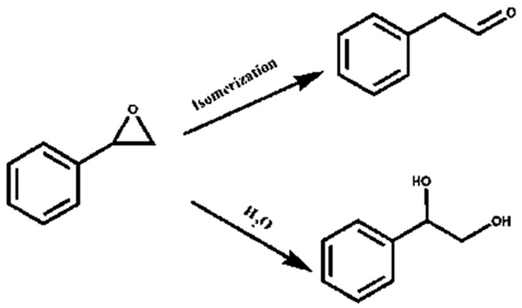

Scheme 1 Possible reaction of the by-product.

Table 2 Cycloaddition reaction of epoxides and CO_2[a]

Entry	Substrate	Product	Conversion (%)	Selectivity (%)
1	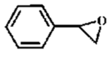	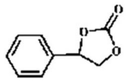	99	99
2	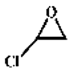	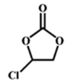	99	99
3	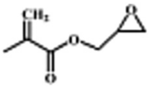	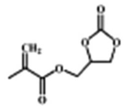	99	94
4	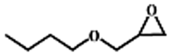	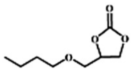	99	99
5[b]	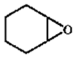	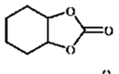	90	89
6	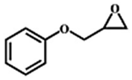	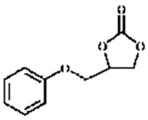	99	99

[a] Reaction conditions: epoxides (5 mmol), 2.5 mol% co-catalyst, catalyst (10 mg), CO_2 pressure (1 atm), reaction time (3 h), conversion and selectivity were determined by GC-MS. [b] Reaction time (5 h).

the co-catalyst, none of the morphology of $Fe_4^{III}(Fe(CN)_6)_3$ resulted in lower conversion and selectivity. Hence, the collaboration of the Lewis acid and nucleophilic agent is necessary to achieve high conversion for this reaction.[46] Furthermore, Table S2 (ESI†) shows a detailed comparison with different reported metal cyanides as high-efficiency catalyst for the cycloaddition reaction.

The differences between three types of co-catalysts are the halide ions; therefore, the performances of the co-catalyst towards the cycloaddition reaction are influenced by the halide anions. The activity decreased in the order of TBAB > TBAI > TBAC. The nucleophilic property ($Cl^- > Br^- > I^-$) and leaving ability ($I^- > Br^- > Cl^-$) of halide anions make TBAB a good co-catalyst.[47]

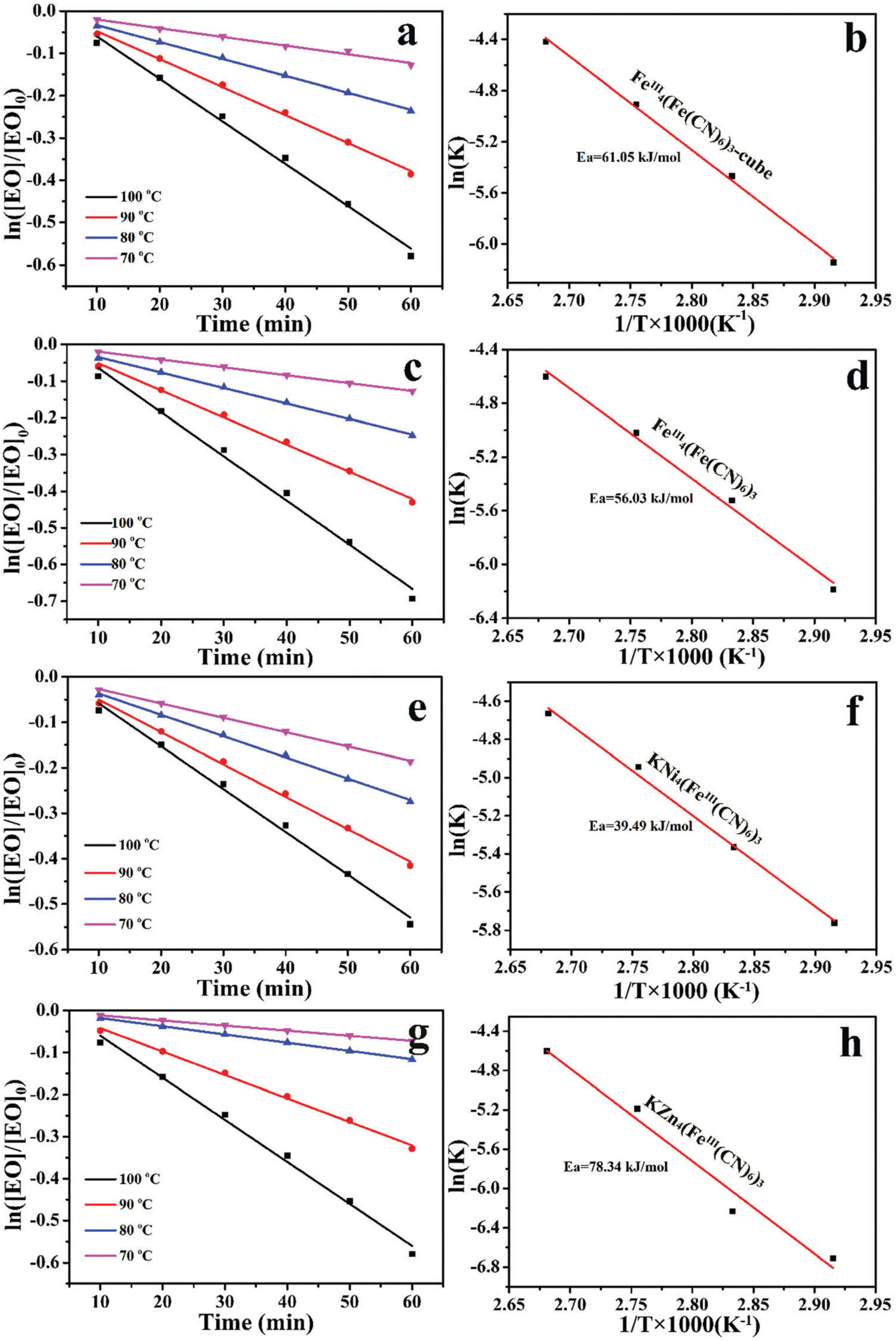

Fig. 5 The reaction rate constant at each temperature (a, $Fe_4^{III}(Fe(CN)_6)_3$), (c, $Fe_4^{III}(Fe(CN)_6)_3$-cube), (e, $KNi_4(Fe^{III}(CN)_6)_3$), (g, $KZn_4(Fe^{III}(CN)_6)_3$) *vs.* the activation energy of catalysts (b, $Fe_4^{III}(Fe(CN)_6)_3$), (d, $Fe_4^{III}(Fe(CN)_6)_3$-cube), (f, $KNi_4(Fe^{III}(CN)_6)_3$), (h, $KZn_4(Fe^{III}(CN)_6)_3$). Reaction conditions: epoxides (5 mmol), 2.5 mol% co-catalyst, catalyst (10 mg), CO_2 pressure (1 atm), conversion was determined by GC-MS.

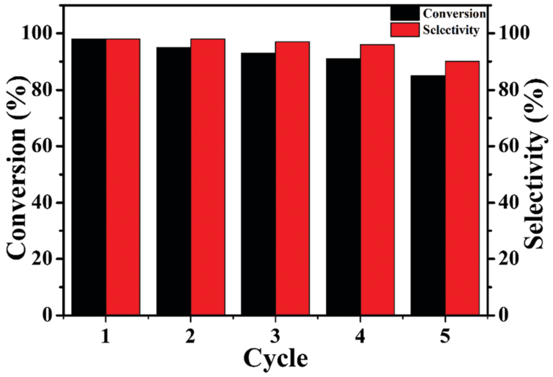

Fig. 7 Reusability of $Fe_4^{III}(Fe(CN)_6)_3$. (Reaction conditions: styrene oxide (5 mmol), 2.5 mol% co-catalyst, catalyst (10 mg), CO_2 pressure (1 atm), reaction time (3 h), conversion and selectivity were determined by GC-MS.)

From the entries (3 and 10–13), we found that the cycloaddition reaction is sensitive towards temperature. When the temperature was decreased from 100 °C to 80 °C, the conversion and selectivity both were found to decrease. The lowest conversion and selectivity was observed when the temperature was 60 °C. A lower reaction temperature produced more by-products with the epoxide ring-opening reaction when the iron cyanide complex was used as a catalyst. Therefore, we can conclude that CO_2 needs a higher temperature. Therefore, it can be concluded that when $Fe_4^{III}(Fe(CN)_6)_3$ is used as the catalyst, a lower reaction temperature is not suitable for the cycloaddition reaction.

For this reaction, the possible by-products are hyacinthin and 1-phenyl-1,2-ethanediol (Scheme 1). Hyacinthin is produced by the isomerization of styrene oxide and 1-phenyl-1,2-ethanediol is produced by the hydrolysis of styrene oxide. For the cycloaddition reaction of styrene oxide with CO_2, the catalyst is an important factor to retard the production of the by-product.[48,49] So, a high activity of the catalyst is beneficial for the cycloaddition reaction. Table 1 shows that $Fe_4^{III}(Fe(CN)_6)_3$ as the catalyst and the 100 °C as the reaction temperature is the best reaction condition for cycloaddition reaction.

To investigate the compatibility of the catalyst, different types of epoxides were chosen for the cycloaddition reaction under 1 atm pressure and 100 °C. Different types of epoxides were converted to relevant products with good conversion and selectivity. In the presence of TBAB as catalyst, the epichlorohydrin showed a high yield of 99%, probably attributed to the electron-withdrawing ability of the chlorine atom.[50] The conversion of cyclohexane oxide was lower, which may have resulted from the steric hindrance (Table 2).[51]

3.3 Kinetic study

To understand the mechanism of the reaction and further investigate the impact of the co-catalyst in the cycloaddition reaction, a kinetic study was carried out for the reaction between styrene oxide and CO_2. The reaction rate is defined as per eqn (1), where, [S] and [Cat] are the concentrations of the substrate and catalysts, k represents the rate constant, and a and b are the series of $[CO_2]$ and [S], respectively. In the process of reaction, the concentration of catalysts and the pressure of CO_2 are not changed, so it can have a change with expression $K = k[CO_2]^a$, so eqn (1) can be simplified to eqn (2). Based on the reported literarure, the reaction of styrene oxide and CO_2 is first order.[52,53] So we can hypothesize that the reaction is a first order reaction, which modifies eqn (2) to eqn (3). According to the Arrhenius equation (eqn (4)) and eqn (5), it can be seen that if the rate constant is known at different temperatures, the activation energy can be calculated, where K is the apparent rate constant of the reaction, A is the pre-exponential factor, E_{act} is the activation energy, R is the ideal gas constant ($8.314\ \text{J mol}^{-1}\ \text{K}^{-1}$) and T is the reaction temperature.

$$-\frac{\mathrm{d[S]}}{\mathrm{d}t} = k[\mathrm{CO_2}]^a[\mathrm{S}]^b \tag{1}$$

$$-\frac{\mathrm{d[S]}}{\mathrm{d}t} = k'[\mathrm{S}]^b \tag{2}$$

$$\ln[\mathrm{S}]_t = -Kt + \ln[\mathrm{S}]_0 \tag{3}$$

$$K = A\mathrm{e}^{-\frac{E_{\text{act}}}{RT}} \tag{4}$$

$$\ln K = \ln A - \frac{E_{\text{act}}}{R}\left(\frac{1}{T}\right) \tag{5}$$

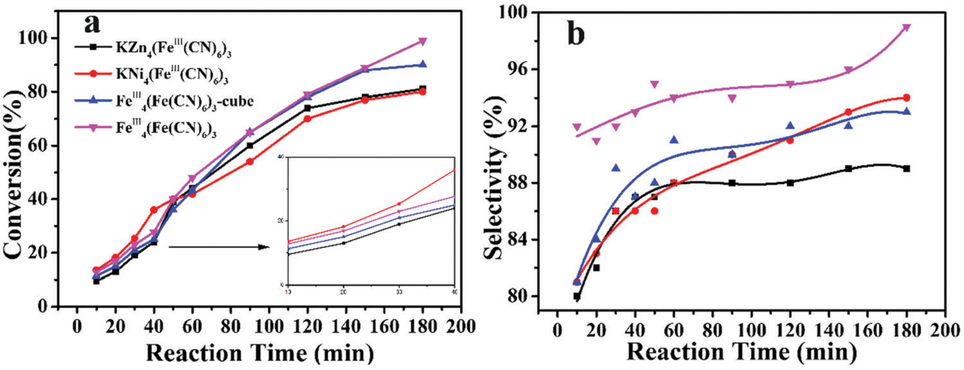

Fig. 6 Conversion (a) and selectivity (b) using different catalysts. Reaction conditions: epoxides (5 mmol), 2.5 mol% co-catalyst, catalyst (10 mg), CO_2 pressure (1 atm), conversion and selectivity were determined by GC-MS.

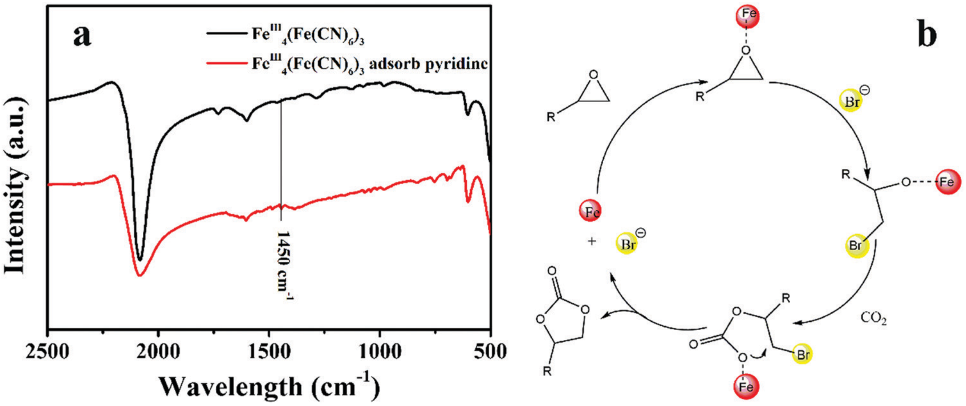

Fig. 8 (a) FTIR spectra of $Fe^{III}_4(Fe(CN)_6)_3$ and pyridine adsorbed $Fe^{III}_4(Fe(CN)_6)_3$, (b) proposed mechanism of the cycloaddition reaction.

The apparent rate constant of different types of catalysts at different temperatures and their activation energy are elaborated in Fig. 5. All the catalysts follow first order reaction. The rate constants of different catalysts at different reaction temperatures are shown in Tables S2–S5 (ESI†). Moreover, it can be found from Fig. 5 that the activation energies of $KNi_4(Fe^{III}(CN)_6)_3$, $Fe^{III}_4(Fe(CN)_6)_3$, $Fe^{III}_4(Fe(CN)_6)_3$-cube and $KZn_4(Fe^{III}(CN)_6)_3$ were 39.49 kJ mol^{-1}, 56.03 kJ mol^{-1}, 61.05 kJ mol^{-1} and 78.34 kJ mol^{-1}, respectively.

Moreover, the conversion efficiency of the catalyst was further evaluated by a thermodynamic study (Fig. 6); the conversion of $KNi_4(Fe^{III}(CN)_6)_3$, $Fe^{III}_4(Fe(CN)_6)_3$, $Fe^{III}_4(Fe(CN)_6)_3$-cube and $KZn_4(Fe^{III}(CN)_6)_3$ are 36%, 28%, 25% and 24%, respectively, with the reaction time being 40 min. Furthermore, the result showed that the data conformed well to the kinetic study: the catalyst with lower activation energy had the higher conversion at the same time. Fig. 6b shows the selectivity of several catalysts, indicating that the selectivity increases with the increase in reaction time. This is because at the beginning of the reaction time, a mass of by-products was produced, and at the end, the product consists mainly of the target product.

3.4 Catalyst recycling

The as-prepared catalyst not only has good catalytic activity but also has good recyclability and reusability.[48] After the reaction, the catalyst was collected with centrifugation and washed with alcohol for three times, and then dried in vacuum. The recycled catalyst was reused for the next reactions. Therefore, a variety of CO_2 and styrene oxide reactions were conducted under solvent free condition at 100 °C and 1 atm pressure. TBAB as the co-catalyst was used during the recyclability and reusability study of the catalyst. The recycling ability of the catalyst is shown in Fig. 7, which shows that after five recycling cycles, the conversion and selectivity decreased only slightly. This result shows that the catalyst has good recyclability and reusability. Finally, after recycling the catalyst for five times, we analyzed the catalyst with ICP and found that the content of Fe reduced from 37.39% to 33.92%, which may be due to centrifugation as well as experimental errors in the recycling experiments.

3.5 Proposed Mechanism

To determine the acid type of the catalyst, infrared spectroscopy (IR) was performed on $Fe^{III}_4(Fe(CN)_6)_3$ and pyridine adsorbed $Fe^{III}_4(Fe(CN)_6)_3$. The pyridine adsorbed $Fe^{III}_4(Fe(CN)_6)_3$ was prepared by mixing 3 mL pyridine and 50 mg $Fe^{III}_4(Fe(CN)_6)_3$ in a round-bottom flask under magnetic stirring for 5 h at room temperature. Then, the catalyst was collected by distillation and dried at 80 °C overnight. The result of the acid type of the catalyst is shown in Fig. 7a. After adsorbing pyridine, a peak was observed at 1450 cm^{-1}, indicating that the catalyst was a Lewis acid.

The catalytic mechanism of the catalyst can be explained by the following steps. First, the epoxide reacts with the Lewis acid followed by a nucleophilic attack on epoxide by TBAB to form a metal alkoxide intermediate.[36,54] After that, CO_2 and the intermediate form an acyclic carbonate. Finally, the cyclic carbonate was produced when the catalyst left the intermediate.[55] From the above mechanism, it could be seen that the Lewis acid and nucleophile work together for this reaction and are necessary for this cycloaddition reaction (Fig. 8).

4. Conclusion

In summary, we report a green and facile method to synthesize a highly active catalyst to catalyze the cyclic reaction between carbon dioxide and epoxides. After the screening of the reaction conditions (CO_2 at atmospheric pressure, solvent free, 100 °C), satisfactory conversion (99%) and selectivity (99%) were obtained. Moreover, the mechanism of the reaction was investigated by kinetic study. In addition, the recyclability test of the catalyst indicates that it could be reused for 5 times without a significant decrease in activity.

Conflicts of interest

There are no conflicts to declare.

Acknowledgements

The authors thank for the financial support from the National Natural Science Foundation of China (No. 21773098).

References

1 Z. Shi, G. Niu, Q. Han, X. Shi and M. Li, *Mol. Catal.*, 2018, **461**, 10–18.

2 Y. Ma, Y. Zhang, C. Chen, J. Zhang, B. Fan, T. Wang, T. Ren, L. Wang and J. Zhang, *Ind. Eng. Chem. Res.*, 2018, **57**, 13342–13352.

3 D. Zheng, J. Zhang, X. Zhu, T. Ren, L. Wang and J. Zhang, *J. CO2 Util.*, 2018, **27**, 99–106.

4 Q. Han, B. Qi, W. Ren, C. He, J. Niu and C. Duan, *Nat. Commun.*, 2015, **6**, 10007.

5 T. Wang, D. Zheng, J. Zhang, B. Fan, Y. Ma, T. Ren, L. Wang and J. Zhang, *ACS Sustainable Chem. Eng.*, 2018, **6**, 2574–2582.

6 Q. Yi, W. Li, J. Feng and K. Xie, *Chem. Soc. Rev.*, 2015, **44**, 5409–5445.

7 A. Sanna, M. Uibu, G. Caramanna, R. Kuusik and M. M. Maroto-Valer, *Chem. Soc. Rev.*, 2014, **43**, 8049–8080.

8 Q. Liu, L. Wu, R. Jackstell and M. Beller, *Nat. Commun.*, 2015, **6**, 5933.

9 M. W. H. Donald and J. Darensbourg, *Coord. Chem. Rev.*, 1996, **153**, 155–174.

10 X. Wang, Y. Zhou, Z. Guo, G. Chen, J. Li, Y. Shi, Y. Liu and J. Wang, *Chem. Sci.*, 2015, **6**, 6916–6924.

11 J. Langanke, A. Wolf, J. Hofmann, K. Böhm, M. A. Subhani, T. E. Müller, W. Leitner and C. Gürtler, *Green Chem.*, 2014, **16**, 1865–1870.

12 S. W. Jîrgen Klankermayer, K. Beydoun and W. Leitner, *Angew. Chem., Int. Ed.*, 2016, **55**, 7296–7343.

13 S. G. Jadhav, P. D. Vaidya, B. M. Bhanage and J. B. Joshi, *Chem. Eng. Res. Des.*, 2014, **92**, 2557–2567.

14 C. A. Huff and M. S. Sanford, *ACS Catal.*, 2013, **3**, 2412–2416.

15 J. W. Comerford, I. D. V. Ingram, M. North and X. Wu, *Green Chem.*, 2015, **17**, 1966–1987.

16 V. Laserna, E. Martin, E. C. Escudero-Adán and A. W. Kleij, *ACS Catal.*, 2017, **7**, 5478–5482.

17 C. J. Whiteoak, N. Kielland, V. Laserna, E. C. Escudero-Adán, E. Martin and A. W. Kleij, *J. Am. Chem. Soc.*, 2013, **135**, 1228–1231.

18 B. Schäffner, F. Schäffner, S. P. Verevkin and A. Börner, *Chem. Rev.*, 2010, **110**, 4554–4581.

19 C. M. Alder, J. D. Hayler, R. K. Henderson, A. M. Redman, L. Shukla, L. E. Shuster and H. F. Sneddon, *Green Chem.*, 2016, **18**, 3879–3890.

20 C. Martín, G. Fiorani and A. W. Kleij, *ACS Catal.*, 2015, **5**, 1353–1370.

21 L.-N. He, H. Yasuda and T. Sakakura, *Green Chem.*, 2003, **5**, 92–94.

22 A. Sibaouih, P. Ryan, M. Leskelä, B. Rieger and T. Repo, *Appl. Catal., A*, 2009, **365**, 194–198.

23 A.-L. Girard, N. Simon, M. Zanatta, S. Marmitt, P. Gonçalves and J. Dupont, *Green Chem.*, 2014, **16**, 2815–2825.

24 S. Zhang, Y. Chen, F. Li, X. Lu, W. Dai and R. Mori, *Catal. Today*, 2006, **115**, 61–69.

25 A. Decortes, M. Martinez Belmonte, J. Benet-Buchholz and A. W. Kleij, *Chem. Commun.*, 2010, **46**, 4580–4582.

26 J.-Q. Wang, W.-G. Cheng, J. Sun, T.-Y. Shi, X.-P. Zhang and S.-J. Zhang, *RSC Adv.*, 2014, **4**, 2360–2367.

27 C. Maeda, T. Taniguchi, K. Ogawa and T. Ema, *Angew. Chem., Int. Ed.*, 2015, **54**, 134–138.

28 M. H. Beyzavi, R. C. Klet, S. Tussupbayev, J. Borycz, N. A. Vermeulen, C. J. Cramer, J. F. Stoddart, J. T. Hupp and O. K. Farha, *J. Am. Chem. Soc.*, 2014, **136**, 15861–15864.

29 Y. Xie, T. T. Wang, X. H. Liu, K. Zou and W. Q. Deng, *Nat. Commun.*, 2013, **4**, 1960.

30 R. J. Herold, *US Pat.*, 3278459, 1966.

31 M. J. Y. Il Kim, K. J. Lee, D.-W. Park and C.-S. H. Bu Ung Kim, *Catal. Today*, 2006, **111**, 292–296.

32 M. J. Y. Il Kim, S. H. Byun, D. W. Park, B. U. Kim and C. S. Ha, *Macromol. Symp.*, 2005, **224**, 181–191.

33 S. Chen, X. Zhang, F. Lin and G. Qi, *React. Kinet. Catal. Lett.*, 2007, **91**, 69–75.

34 Z.-J. H. Xing-Hong Zhang, S. Chen, F. Liu and G.-R. Q. Xue-Ke Sun, *Appl. Catal., A*, 2007, **325**, 91–98.

35 D. J. Darensbourg, M. J. Adams and J. C. Yarbrough, *Inorg. Chem.*, 2001, **40**, 6543–6544.

36 M. M. D. Jose Tharun, Y. Hwang, R. Roshan, M. S. Park and D.-W. Park, *Appl. Catal., A*, 2012, **419–420**, 178–184.

37 L. Zhang, H. B. Wu and X. W. Lou, *J. Am. Chem. Soc.*, 2013, **135**, 10664–10672.

38 T. Liu, X. Niu, L. Shi, X. Zhu, H. Zhao and M. Lana, *Electrochim. Acta*, 2015, **176**, 1280–1287.

39 L. Samain, B. Gilbert, F. Grandjean, G. J. Long and D. Strivay, *J. Anal. At. Spectrom.*, 2013, **28**, 524.

40 M. M. Barsan, I. S. Butler, J. Fitzpatrick and D. F. R. Gilson, *J. Raman Spectrosc.*, 2011, **42**, 1820–1824.

41 L. Liang, Q. Zhu, T. Wang, F. Wang, J. Ma, L. Jing and J. Sun, *Microporous Mesoporous Mater.*, 2014, **197**, 221–228.

42 P. Jiang, X. Li, W. Gao, X. Wang, Y. Tang, K. Lan, B. Wang and R. Li, *Catal. Commun.*, 2018, **111**, 6–9.

43 X. Chen, L. Zhang, B. Zhang, X. Guo and X. Mu, *Sci. Rep.*, 2016, **6**, 28558.

44 J.-Y. Su, G.-P. Jin, T. Chen, X.-D. Liu, C.-N. Chen and J.-J. Tian, *Electrochim. Acta*, 2017, **230**, 399–406.

45 V. V. Nemoshkalenko, K. B. Yatsimirskii, Y. P. Nazarenko, V. G. Aleshin, V. V. Zhilinskaya and N. A. Tomashevsky, *J. Electron Spectrosc. Relat. Phenom.*, 1977, **10**, 239–245.

46 A. Barthel, Y. Saih, M. Gimenez, J. D. A. Pelletier, F. E. Kühn, V. D'Elia and J.-M. Basset, *Green Chem.*, 2016, **18**, 3116–3123.

47 N. Tenhumberg, H. Büttner, B. Schäffner, D. Kruse, M. Blumenstein and T. Werner, *Green Chem.*, 2016, **18**, 3775–3788.

48 Z.-Z. Yang, L.-N. He, C.-X. Miao and S. Chanfreau, *Adv. Synth. Catal.*, 2010, **352**, 2233–2240.

49 F. C. Ya Du, D.-L. Kong and L.-N. He, *Green Chem.*, 2005, **7**, 518–523.

50 L. Wang, K. Kodama and T. Hirose, *Catal. Sci. Technol.*, 2016, **6**, 3872–3877.

51 R. Luo, X. Zhou, Y. Fang and H. Ji, *Carbon*, 2015, **82**, 1–11.

52 R. Luo, W. Zhang, Z. Yang, X. Zhou and H. Ji, *J. CO2 Util.*, 2017, **19**, 257–265.

53 M. Liu, B. Liu, S. Zhong, L. Shi, L. Liang and J. Sun, *Ind. Eng. Chem. Res.*, 2015, **54**, 633–640.

54 J. Chen, M. Zhong, L. Tao, L. Liu, S. Jayakumar, C. Li, H. Li and Q. Yang, *Green Chem.*, 2018, **20**, 903–911.

55 J. Sun, S.-i. Fujita, F. Zhao and M. Arai, *Green Chem.*, 2004, **6**, 613.